J Therm Anal Calorim (2010) 100:225–232
DOI 10.1007/s10973-009-0629-8

Curing reaction of *o*-cresol-formaldehyde epoxy/LC epoxy(*p*-PEPB)/anhydride(MeTHPA)

Cure kinetics and molecular mechanism

Jungang Gao · X. Zhang · L. Huo · H. Zhao

Received: 19 June 2009 / Accepted: 1 December 2009 / Published online: 13 January 2010

Abstract The curing kinetics of a bi-component system about *o*-cresol-formaldehyde epoxy resin (*o*-CFER) modified by liquid crystalline *p*-phenylene di[4-(2,3-epoxypropyl) benzoate] (*p*-PEPB), with 3-methyl-tetrahydrophthalic anhydride (MeTHPA) as a curing agent, were studied by non-isothermal differential scanning calorimetry (DSC) method. The relationship between apparent activation energy E_a and the conversion α was obtained by the isoconversional method of Ozawa. The reaction molecular mechanism was proposed. The results show that the values of E_a in the initial stage are higher than other time, and E_a tend to decrease slightly with the reaction processing. There is a phase separation in the cure process with LC phase formation. These curing reactions can be described by the Šesták–Berggren (S–B) equation, the kinetic equation of cure reaction as follows: $\frac{d\alpha}{dt} = A\exp\left(-\frac{E_a}{RT}\right)\alpha^m(1-a)^n$.

Keywords Activation energy · Reaction mechanism · Liquid crystal · Epoxy resins · Curing kinetics

Introduction

Epoxy resins are widely used in the polymer industry as coatings, structural adhesives, insulating materials, and polymeric composite materials, etc. The *o*-cresol-formaldehyde epoxy resin (*o*-CFER, Scheme 1) is considered worthy of further study in terms of their good chemical resistance, electric properties, and mechanical properties. The studies of the applications and physical properties of *o*-CFER have been reported in recent years [1]. However, it is also limited in many high-performance applications because of their brittleness and lower thermal resistance. The most factors that influence these properties of epoxy resins are the structure of molecular chain and morphology. Recently, epoxy resins had been efficiently toughened and increasing thermal stability via blending with thermoplastics, elastomers, and organic/inorganic hybrid technology [2–5].

Liquid crystal (LC) materials have great potential for functional molecular systems because of their self-organized dynamic structure. Thermotropic LC compound is a sort of LC compounds and which has become important in the field of advanced materials, such as electronic devices and high-strength fibers. Recently many studies have been focused on LC polymer networks by polymerization of liquid crystal monomers [6, 7]. The macroscopically oriented polymer networks are found to exhibit anisotropic mechanical properties, optical property, unique thermal property, and can improve processability of polymeric materials.

The liquid crystalline epoxy resins (LCER) show interesting properties due to the combination of thermoset and LC formation capability [8–10]. As compared with the commercial epoxy resins, crosslinked LC epoxy resin exhibit higher fracture toughness and mechanical properties when oriented by magnetic fields [11, 12]. Recently, it has been recognized that these properties of epoxy resins could be greatly enhanced if liquid crystalline structures are incorporated into the epoxy networks [7, 13, 14]. However, there are no reports about the modified properties of *o*-CFER with LC epoxy resin until now.

The physical and mechanical properties of epoxy polymeric materials intensely depend on the curing process, so the studies of cure kinetics for epoxy resins become

J. Gao (✉) · X. Zhang · L. Huo · H. Zhao
College of Chemistry and Environmental Science, Hebei University, 071002 Baoding, China
e-mail: gaojg@mail.hbu.edu.cn

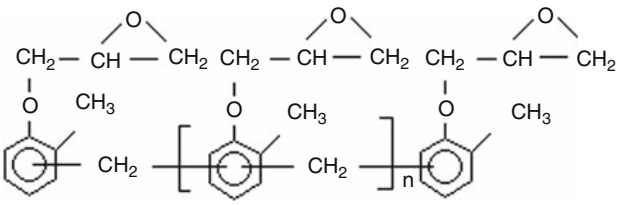

Scheme 1 The molecular structure of *o*-CFER

important. The methods used to study the cure kinetics can be classified as mechanistic and phenomenological. Mechanistic model is made from the balance of chemical species involved in the chemical reaction. In most cases, it is difficult to derive a mechanistic model because the curing reaction of epoxy resin is very complex. Thus, phenomenological or empirical models are preferred to study the cure kinetics of these polymers. One of these methods is non-isothermal differential scanning calorimetry (DSC) method and the relationship between apparent activation energy E_a with the conversion α was obtained by the isoconversional method [15, 16].

In this work, the *o*-CFER was modified by *p*-PEPB as a LC epoxy resin, and the cure kinetics of *o*-CFER/*p*-PEPB/MeTHPA system was investigated by non-isothermal DSC at different heating rates. The dependencies of the apparent activation energy E_a with the conversion α were revealed overall the curing reaction by the Ozawa's method [17]. Some parameters were obtained according to Šesták–Berggren (S–B) equation [18, 19]. The molecular mechanism of curing reaction was proposed.

Experimental

Materials

Epichlorohydrin, *o*-cresol, formaldehyde, 3-methyl-tetrahydrophthalic anhydride (MeTHPA), hydrochloric acid, *N*,*N*′-dimethyl-benzylamine (DMBA), hydroquinone, 4-hydroxy ethyl benzoate, sulfoxide chloride, *m*-chloroperoxybenzoic acid (MCPBA), tetrahydrofuran (THF), and *N*,*N*′-dimethylformamide (DMF) are all analytically pure grade and supplied by the Tianjin Chemical Reagent Co. China. Allyl bromide was supplied by Jiangsu, Fangqiao Chem. Co. China. The *o*-CFER was synthesized according to literatures [1, 2], the structure as Scheme 1 and epoxy value is 0.401 mol/100 g. The *p*-PEPB was synthesized from 4-hydroxy ethyl benzoate, hydroquinone, allyl bromide, and MCPBA according to literatures [20, 21], the melting point is 180 °C, clear point is 250 °C, and the epoxy value is 0.401 mol/100 g. The formation and structure of *p*-PEPB can be described as Scheme 2.

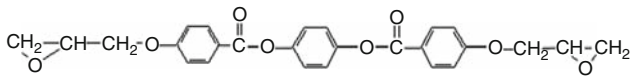

Scheme 2 The molecular structure of *p*-PEPB

Preparation of sample and characterization

Five samples were prepared according to mass percent of *p*-PEPB in total epoxy resin: 0% (No. 1), 10% (No. 2), 20% (No. 3), 50% (No. 4), and 100% (No. 5). The *o*-CFER and *p*-PEPB was mixed homogeneously and heated to melt and cold to room temperature, then the MeTHPA with a stoichiometric ratio of one epoxy group to one carboxy group was added to the system with 0.1% DMBA. Curing reactions were carried out on a differential scanning calorimeter (DSC, Diamond, Perkin Elmer Co. USA). The DSC instrument was calibrated with high-purity indium. Approximately 5 mg sample in a standard aluminum pan was heated at 5, 10, 15, 20 °C/min from 20 to 250 °C under an atmosphere of N_2, respectively.

Results and discussion

The E_a and molecular mechanism of curing reaction

The cure kinetics for all five samples were measured by the non-isothermal DSC method at a heating rate of 5, 10, 15, and 20 °C/min, respectively. The curing thermograms of *p*-PEPB/*o*-CFER/MeTHPA (No. 4) system are shown in Fig. 1. As seen from Fig. 1, the exothermic peaks are attributed to the curing reaction of this system. The heating rate shows a great influence on the curing process. The initial curing temperature (T_{icu}), the peak temperature (T_{pcu}), and the finishing temperature (T_{fcu}) increased with the heating rate, and the temperature range of curing reaction is broaden in evidence. The DSC curves of the

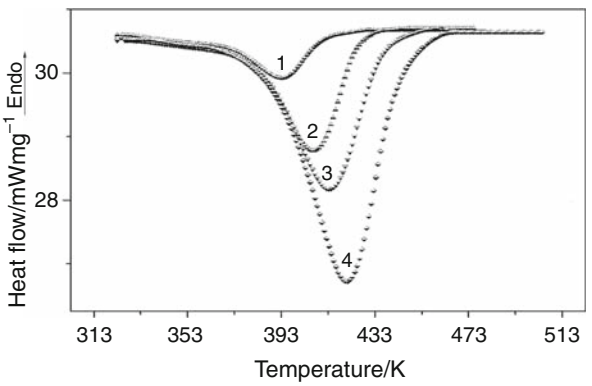

Fig. 1 The cure curve of *p*-PEPB/*o*-CFER/MeTHPA (No. 4) 1–5 K/min; 2–10 K/min; 3–15 K/min; 4–20 K/min

p-PEPB/*o*-CFER/MeTHPA are all very smooth and only show one evident curing peak at a heating rate. The results illuminate that the compatibility of this system is very well and can co-cure. The similar result can be obtained for other samples under the same condition.

From the plots of the initial temperature (T_{icu}), the peak temperature(T_{pcu}), and the finishing temperature (T_{fcu}) versus heating rate β, we can obtain that the gel temperature of cured-system T_{gel}, curing peak temperature T_{pcu} and disposal temperature T_{fcu} at $\beta = 0$, respectively (shown in Table 1). As seen from Table 1, the T_{gel}, T_{pcu}, and T_{fcu} about *p*-PEPB/MeTHPA system are usually higher than bi-component systems of *p*-PEPB/*o*-CFER/MeTHPA and increasing with *p*-PEPB is added to the blend at $\beta = 0$, but *o*-CFER/MeTHPA (No. 1) has a higher T_{fcu} than *p*-PEPB/*o*-CFER/MeTHPA systems. It is illuminated that *o*-CFER/MeTHPA has a higher fully curing temperature.

For non-isothermal curing process, the isoconversional method can be expressed in several ways. The Eq. 1 is known as the Ozawa's method [17, 22, 23], which can be applied to different conversion α of curing process. Thus, for a given α, the E_a can be obtained from linear regression according to Eq. 1.

$$\ln \beta = A' - 1.052\frac{E_a}{RT} \quad (1)$$

where A' is the pre-exponential factor of Arrhenius equation, T is the temperature (K), R is the gas constant (8.314 J mol/K), β is heating rate, E_a is the apparent activation energy, $A' = \lg AE_a/g(\alpha)R - 3.315$ and $g(\alpha) = \int_0^\alpha \frac{d\alpha}{f(\alpha)} = \frac{A}{\beta}\int_0^T \exp(-E_a/RT)dT$.

Table 1 Data of T_{gel}, T_{pcu}, and T_{fcu} for different samples

Sample	Property	Heating rate/K min^{-1}				
		0	5	10	15	20
No. 1	T_{gel}	86.06	87.20	88.87	89.92	91.16
	T_{pcu}	117.32	123.45	134.76	141.72	147.02
	T_{fcu}	152.17	159.68	173.81	181.62	188.83
No. 2	T_{gel}	93.63	98.48	103.72	109.94	113.43
	T_{pcu}	118.35	125.01	136.54	143.78	149.86
	T_{fcu}	138.64	151.47	160.94	178.93	186.60
No. 3	T_{gel}	96.15	98.26	100.01	102.14	104.24
	T_{pcu}	118.11	124.40	133.65	140.85	146.23
	T_{fcu}	137.46	147.86	159.39	168.82	180.20
No. 4	T_{gel}	96.72	98.48	100.83	102.78	104.35
	T_{pcu}	131.55	135.07	141.61	145.96	148.65
	T_{fcu}	144.55	154.30	162.24	173.58	181.74
No. 5	T_{gel}	108.25	110.19	112.74	114.83	116.63
	T_{pcu}	131.50	136.39	144.17	149.03	153.96
	T_{fcu}	154.09	164.51	173.42	183.75	194.26

The relationships between α and dynamic curing temperature T for *p*-PEPB/*o*-CFER/MeTHPA (No. 4) system are shown in Fig. 2.

As seen from Fig. 2, at the same α value, the isoconversional temperature T increased with the heating rate. According to α–T and Ozawa equation 1, from the plots of $\ln\beta$ vs. $1/T$, the E_a at any conversion α can be calculated, the linear coefficients are all between 0.9923 and 0.9991, and it shows that the curing systems well obey for Ozawa's kinetics model. According to the same method, the relationships of E_a with α can be obtained for other four samples. Figure 3 shows the variation of E_a with α for five samples in the interval of $0 \leq \alpha \leq 1$.

As seen from Fig. 3, the E_a values change when α change, it is because the mechanism of curing reaction for epoxy/MeTHPA is complex due to gelation, vitrification, and phase change for LC system. The *p*-PEPB/MeTHPA system has a higher E_a than other systems, and the E_a increase with increasing of *p*-PEPB content. The reason is that the *p*-PEPB can form LC texture in the cure process because of the self-congregation, and the LC texture will

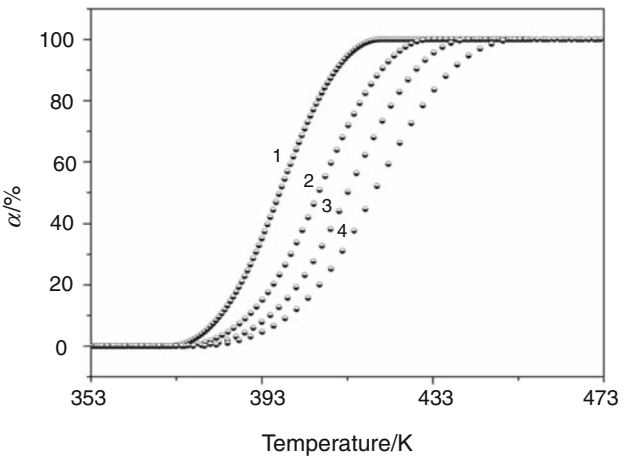

Fig. 2 Relationship of α of sample No. 4 versus temperature T. 1–5 K/min; 2–10 K/min; 3–15 K/min; 4–20 K/min

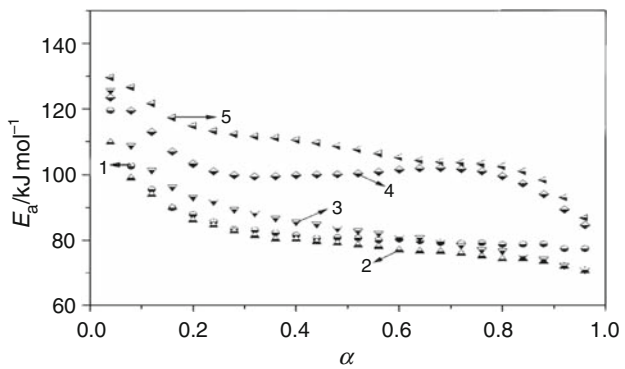

Fig. 3 Relationship of E_a versus α for five samples. *1* No. 1; *2* No. 2; *3* No. 3; *4* No. 4; *5* No. 5

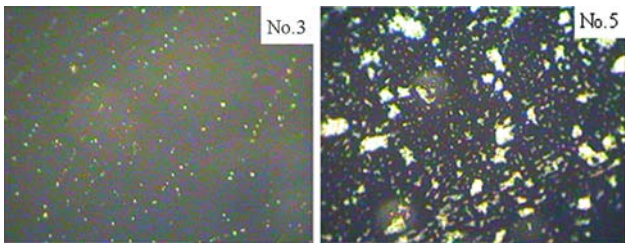

Fig. 4 The POM photographs (×400) of No. 5 and No. 3

induce a larger steric effects and higher reaction activation barrier. But when the *p*-PEPB content is lower (as No. 2 and No. 3), the E_a is lower than that of pure *o*-CFER/MeTHPA in final stage of curing reaction. The reason is that the *p*-PEPB induced only tiny phase separation in the curing process, and may decrease the viscosity of reaction system. The POM photographs of the morphology texture of *p*-PEPB/MeTHPA (No. 5) and *p*-PEPB/*o*-CFER/MeTHPA (No. 3) are shown in Fig. 4 (No. 5 and No. 3). As seen from Fig. 4 (No. 3), the bi-component system had formed phase separation of liquid crystal and taken on a structure of sea-island. This is because of the liquid crystalline molecules have a larger tendency of self-conglomeration than with *o*-CFER molecules. It shows that the morphological structure of epoxy resin is improved by the addition of the LC epoxy resin. The LC phase appears as fiber and granule in the core section of this blend. The presence of these LC fiber and granule could alleviate the stress concentration, and come into bring slippage cingulums and crakes in the process of fraction. So the toughness of blends is improved through the addition of small amounts of the LC epoxy resin, and the mechanical and thermal properties are enhanced [15].

The values of E_a in the initial stage (α = 0–0.15) are higher than those of any other time for all samples, then E_a tend to decrease slightly with the reaction processing and only have very little variation for conversions between $0.3 \leq \alpha \leq 0.8$ (except for No. 5 and No. 3). The molecular mechanisms of the curing reaction are proposed in Scheme 3. As seen from Scheme 3, the higher E_a in the initial stage shows that the opening ring reaction of MeTHPA with oxygen anion or N in DMBA has a higher E_a (b or c) than that of reaction of carboxy anion with epoxy group (a). This is because of the MeTHPA is a stable five-member ring structure and has a p–π resonance nature, but epoxy ring is an unstable three-member ring. On the other hand, the E_a of mixing systems are all lower than that of *p*-PEPB/MeTHPA system, this is because, that the some hydroxyl group is existed in the *o*-CFER molecule, and can form a hydroxyl catalyzed transition state with epoxy group (d) or MeTHPA (e) which can decrease E_a. In the final stage ($\alpha > 0.8$) except for No. 1, the curing E_a decrease, which is attributed to formation of liquid crystalline phase and gelation [24].

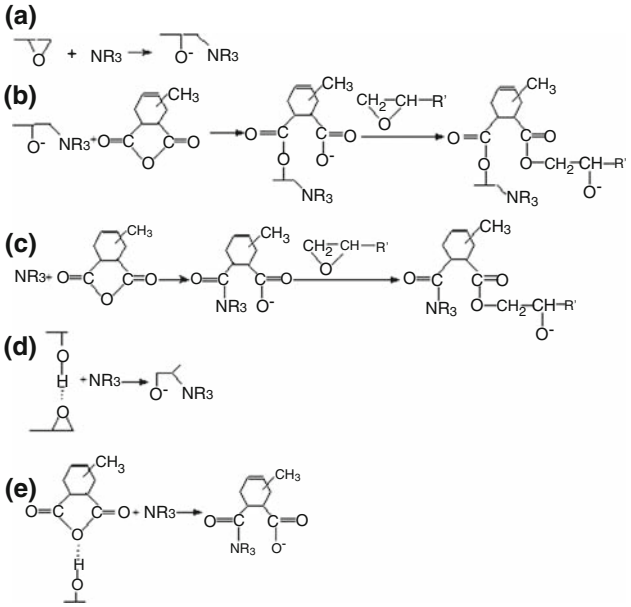

Scheme 3 The reaction mechanism of epoxy resins with MeTHPA using tertiary amine as a catalyst

Non-isothermal cure kinetics

The basic assumption for the application of DSC technique to the thermosets, the rate of curing reaction ($d\alpha/dt$) is proportional to the measured heat flow $\phi = dH/dt$

$$\frac{d\alpha}{dt} = \frac{dH}{dt} \cdot \frac{1}{\Delta H} \tag{2}$$

where ΔH is the enthalpy of the curing reaction, and $d\alpha/dt$ is defined as curing rate. The reaction rate of curing process can be described as follows:

$$\frac{d\alpha}{dt} = k(T)f(\alpha) \tag{3}$$

where $k(T)$ is a temperature-dependent reaction rate constant, and follows an Arrhenius equation, $f(\alpha)$ is a temperature-dependent kinetic model function.

Then the values of E_a obtained from Ozawa's method can be used to find the appropriate kinetic model which best describes the conversion function $f(\alpha)$ of this curing process [18, 22]. The most suitable kinetic model can be evaluated with the functions $y(\alpha)$ and $z(\alpha)$ according to the Eqs. 4 and 5 as follows:

$$y(\alpha) = \frac{d\alpha}{dt} \cdot \exp(x) \tag{4}$$

$$z(\alpha) = \pi(x) \cdot \left(\frac{d\alpha}{dt}\right) \cdot \frac{T}{\beta} \tag{5}$$

where x is reduced activation energy ($x = E_a/RT$), $\pi(x)$ is the expression of the temperature integral, which can be well approximated using the fourth rational expression as in Eq. 6

$$\pi(x) = \frac{x^3 + 18x^2 + 88x + 96}{x^4 + 20x^3 + 120x^2 + 240x + 120} \quad (6)$$

The $y(\alpha)$ function is proportional to $f(\alpha)$ function, being characteristic for a given kinetic model. The shape and the maximum of both $y(\alpha)$ and $z(\alpha)$ function for several models, are normalized within (0, 1) range. The maximum α_M of the $y(\alpha)$ function and α_P^∞ of the $z(\alpha)$ function suggest the choice of the most suitable kinetic model characterizing the curing process [14, 21].

Using the value of E_a and knowing the kinetic model, the pre-exponential factor A is calculated according to Eq. 3

$$A = -\frac{\beta x_p}{Tf'(\alpha_p)}\exp(x_p) \quad (7)$$

where $f'(\alpha)$ is the differential form of the kinetic model $df(\alpha)/d\alpha$, α_p is the conversion corresponding to the peak on DSC curve.

The average value of E_a was used to calculate both $y(\alpha)$ and $z(\alpha)$ functions, using Eqs. 4 and 5, respectively. The Figs. 5 and 6 show the variation of $y(\alpha)$ and $z(\alpha)$ values with α for sample of No. 3 at different heating rates, respectively. The values of both $y(\alpha)$ and $z(\alpha)$ were normalized within the (0, 1) range. From Figs. 5 and 6, the value of α_M and α_P^∞ (the value of α while $y(\alpha)$ or $z(\alpha)$ get the maximum value of DSC peak, respectively) of No. 3 can be obtained, respectively. According to the same method, the values of α_p, α_M, and α_p^∞ for other four samples can be obtained (Table 2).

As can be noted from Table 2, the values of α_M are lower than the value of α_p, whereas α_p^∞ exhibits values lower than 0.632. In accordance with the results of Málek on the kinetics of the curing reaction of epoxy resins under non-isothermal conditions [18], the studied curing systems all can be described using the two-parameter autocatalytic kinetic model of Šesták–Berggren equation [18, 19, 22].

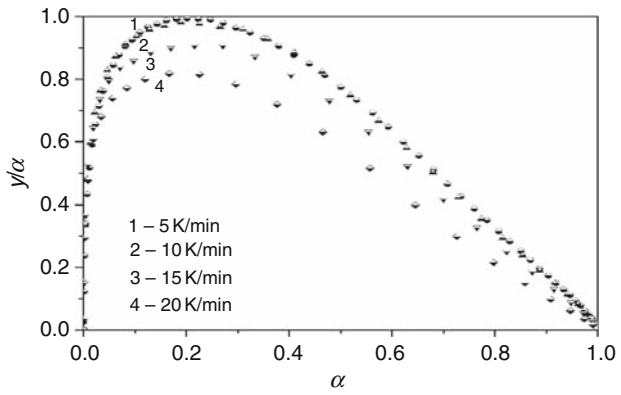

Fig. 5 Variation of $y(\alpha)$ function versus α of No. 3 at different heating rates

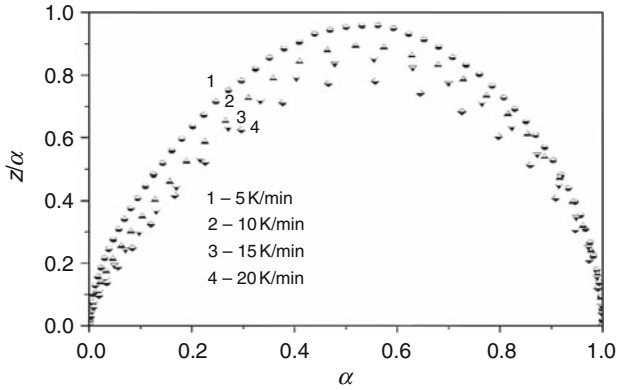

Fig. 6 Variation of $z(\alpha)$ function versus α of No. 3 at different heating rates

Table 2 α_p, α_M, and α_p^∞ values evaluated with the DSC data of five samples

Sample	Heating rate/K min^{-1}	α_p	α_M	α_p^∞
No. 1	5	0.5349	0.1503	0.5177
	10	0.5984	0.0703	0.5907
	15	0.5031	0.0636	0.5202
	20	0.4576	0.0596	0.5688
No. 2	5	0.5159	0.2068	0.5307
	10	0.5233	0.1479	0.5829
	15	0.5163	0.1253	0.5547
	20	0.5328	0.1018	0.5328
No. 3	5	0.5128	0.1949	0.5437
	10	0.5082	0.1857	0.5359
	15	0.5211	0.2709	0.5092
	20	0.5022	0.2006	0.5297
No. 4	5	0.6039	0.0859	0.6287
	10	0.6793	0.0575	0.6158
	15	0.6027	0.0601	0.5984
	20	0.5646	0.0509	0.5812
No. 5	5	0.4707	0.3395	0.4746
	10	0.4779	0.3423	0.4854
	15	0.4485	0.3387	0.4485
	20	0.4459	0.3424	0.4196

$$f(\alpha) = \alpha^m(1-\alpha)^n \quad (8)$$

where m and n are the curing reaction orders.

The kinetic parameter n is obtained by the slope of the linear dependence $\ln[(d\alpha/dt)\cdot e^x]$ vs. $\ln[\alpha_p\cdot(1-\alpha)]$ (from Eq. 3), and $m = pn$, where p is equal to $\alpha_M/(1-\alpha_M)$. Table 3 lists some kinetic parameters evaluated for the proposed Šesták–Berggren kinetic model. The linear correlation coefficients of kinetic parameters in Table 3 are all included between 0.9921 and 0.9993. As it is shown in

Table 3 Kinetic parameters evaluated for five samples

Sample	Heating rate/K min^{-1}	E_a/kJ mol^{-1}	ln$A$	Mean	n	Mean	m	Mean
No. 1	5	83.91	29.21	28.93	1.49	1.35	0.26	0.13
	10		28.91		1.34		0.10	
	15		28.83		1.30		0.09	
	20		28.76		1.28		0.08	
No. 2	5	72.01	28.27	27.96	1.45	1.28	0.38	0.23
	10		27.96		1.18		0.21	
	15		27.89		1.22		0.17	
	20		27.73		1.25		0.14	
No. 3	5	85.33	29.69	29.78	1.10	1.26	0.27	0.35
	10		29.71		1.12		0.26	
	15		30.03		1.42		0.53	
	20		29.68		1.38		0.35	
No. 4	5	100.94	33.75	33.65	0.95	0.80	0.09	0.16
	10		33.66		0.75		0.05	
	15		33.55		0.68		0.04	
	20		33.63		0.81		0.04	
No. 5	5	107.35	37.33	37.46	2.59	2.74	1.33	1.42
	10		37.51		2.73		1.42	
	15		37.49		2.78		1.42	
	20		37.49		2.86		1.49	

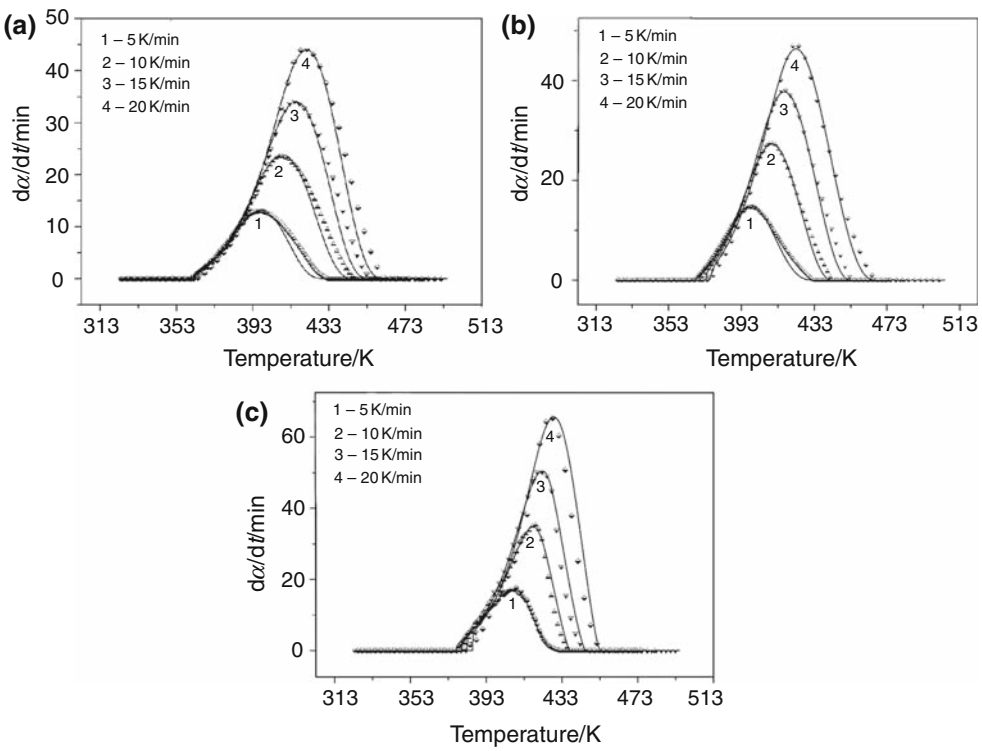

Fig. 7 Comparison of experimental (*symbols*) and calculated (*full lines*) DSC curves for **a** No. 1, **b** No. 2, and **c** No. 4

Table 3, the variation of the kinetic parameters with the heating rate is placed in the experimental error limit (within 10% of the average value).

The correctness of the kinetic model proposed using the S–B equation was verified by plotting dα/dt versus T (experimental dots) with theoretical curves (full lines),

using the data listed in Table 3. Figure 7 presents a comparison of experimental and theoretical values for three samples of the five samples. As seen from Fig. 7, a good agreement can be seen between the calculated theoretical curves and those experimentally determined. But some deviation appears at the last stage, and which is more evident at faster heating rate. This phenomenon was also discovered in other epoxy systems [25–27]. However, it has some different from isothermal DSC, in which the experimental curves are usually lower than theoretical curves at the last stage; whereas in this non-isothermal process, the experimental curves are higher than theoretical curves. In the isothermal process, the deviation is due to the onset of gelation and vitrification, where the mobility of reactive groups is hindered, and the rate of conversion is controlled by diffusion rather than by kinetic factors [9, 28]. But in non-isothermal process, the temperature of samples increase gradually with time, and the free volume of materials and molecular activity increase with temperature simultaneous. In this condition, the diffusion rate and kinetic energy of reactive groups enhance, and leading to increase reaction rate. So, the experimental curves may be higher than theoretical curves at the last stage. But in Fig. 7, the (c) No. 4 is different with (a) No. 1 and (b) No. 2, in which the experimental curves are lower than theoretical curves at the last stage, which may attribute that the more LC phase is formed and higher crosslink in this system. But the two-parameter S–B model can still give a well description for all the studied curing systems, and these systems follow the kinetic equation:

$$\frac{\mathrm{d}\alpha}{\mathrm{d}t} = A\exp\left(-\frac{E_a}{RT}\right)\alpha^m(1-a)^n \qquad (9)$$

Conclusions

The cure kinetics of *p*-PEPB/MeTHPA and *p*-PEPB/*o*-CFER/MeTHPA systems can all be described by Ozawa equation. The E_a of *p*-PEPB/MeTHPA is 107.35 kJ mol^{-1} and it is higher than that of mixing systems of *p*-PEPB/*o*-CFER/MeTHPA (the average E_a is 72–101 kJ mol^{-1}, different according to content of *p*-PEPB). The LC phase can be formed in the curing process for pure LC and mixing systems.

The non-isothermal cure kinetics of these systems can all be described by two-parameter (*m*, *n*) Šesták–Berggren autocatalytic kinetic model. The DSC experimental results have some deviation with those theoretically calculated ones at last stage of curing reaction at higher heating rates. The reaction orders *n* and *m* for *p*-PEPB/MeTHPA are 2.74, 1.42, respectively, but it has different values to *p*-PEPB/*o*-CFER/MeTHPA system with different *p*-PEPB content.

Acknowledgements This article is the project supported by Natural Science Foundation (B2005000108) of Hebei Province, China.

References

1. Akira I, Takeaki S, Yoshiji M, Haruhiko F, Hiroshi U. Hardening organic resin composition. Jpn Kokai Tokkyo Koho 2002; 2002080727.
2. López J, Rico M, Montero B, Díez J, Ramírez C. Polymer blends based on an epoxy-amine thermoset and a thermoplastic: Effect of thermoplastic on cure reaction and thermal stability of the system. J Therm Anal Calorim. 2009;95:369–76.
3. Ramírez C, Rico M, Barral L, Díez J, García-Garabal S, Montero B. Organic/inorganic hybrid materials from an epoxy resin cured by an amine silsesquioxane. J Therm Anal Calorim. 2007;87:69–72.
4. Sharma P, Choudhary V, Narula AK. Curing kinetics and thermal stability of diglycidyl ether of bisphenol: Mixture of aromatic imide-amines of benzophenone 3,3′,4,4′-tetra-carboxylic acid dianhydride and 4,4′-diaminodiphenylsulfone. J Therm Anal Calorim. 2008;91:231–6.
5. Villanueva M, Martín-Iglesias JL, Rodríguez-Añón JA, Proupín-Castiñeiras J. Thermal study of an epoxy system DGEBA ($n = 0$)/mXDA modified with POSS. J Therm Anal Calorim. 2009;96:575–82.
6. Jahromi S, Kuipers WAG, Norder B, Mijs WJ. Liquid crystalline epoxide thermosets: dynamic mechanical and thermal properties. Macromolecules. 1995;28:2201–11.
7. Hoyle CE, Watanab T, Whitehead J. Anisotropic network formation by photopolymerization of liquid crystal monomers in a low magnetic field. Macromolecules. 1994;27:6581–8.
8. Kurihara S, Iwamoto K, Nonaka T. Preparation and structure of polymer networks by polymerization of liquid crystalline monomers in DC electric field. Polymer. 1998;39:3565–9.
9. Zhao H, Gao JG, Li YF, Shen SG. Curing kinetics and thermal property characterization of bisphenol-F epoxy resin and MeTHPA system. J Therm Anal Calorim. 2003;74:227–36.
10. Braun D, Frick G, Grell M, Klimes M, Wendorff JH. Liquid crystal/liquid-crystalline network composite systems structure formation and electro-optic properties. Liq Cryst. 1992;11: 929–39.
11. Kurihara S, Sakamoto A, Nonaka T. Liquid-crystalline polymer networks: effect of cross-linking on the stability of macroscopic molecular orientation. Macromolecules. 1999;32:3150–3.
12. Giamberini M, Amendola E, Carfagna C. Liquid crystalline epoxy thermosets. Mol Cryst Liq Cryst. 1995;266:9–22.
13. Zhang BL, Tang GL, Shi KY, You YC, Du ZJ, Huang J. A study on the properties of epoxy resin toughened by a liquid crystal-type oligomer. J Appl Polym Sci. 1999;71:177–84.
14. Bae J, Jang J, Yoon SH. Cure behavior of the liquid-crystalline epoxy/carbon nanotube system and the effect of surface treatment of carbon fillers on cure reaction. Macromol Chem Phys. 2002;203:2196–3204.
15. Perrin FX, Nguyen TH, Vernet JL. Kinetic analysis of isothermal and nonisothermal epoxy-amine cures by model-free isoconversional methods. Macromol Chem Phys. 2007;208:718–29.
16. Vyazovkin S, Sbirrazzuoli N. Kinetic methods to study isothermal and nonisothermal epoxy-anhydride cure. Macromol Chem Phys. 1999;200:2294–3303.
17. Atarsia A, Boukhili R. Relationship between isothermal and dynamic cure of thermosets via the isoconversion representation. Polym Eng Sci. 2000;40:607–20.
18. Málek J. The kinetic analysis of non-isothermal data. Thermochim Acta. 1992;200:257–69.

19. Šesták J, Berggren G. Study of the kinetics of the mechanism of solid-state reactions at increasing temperatures. Thermochim Acta. 1971;3:1–12.
20. Jahromi S, Lub J, Mol GN. Synthesis and photoinitiated polymerization of liquid crystalline diepoxides. Polymer. 1994;35:622–9.
21. Liu XD, Gao JG, Luo QJ, Zhang XN, Wang YY. Synthesis and characterization of p-phenylene di-4-(allyloxy) benzoate. J Hebei Univ (nature). 2007;27:54–8.
22. Rosu D, Mititelu A, Cascaval CN. Cure kinetics of a liquid-crystalline epoxy resin studied by non-isothermal data. Polym Test. 2004;23:209–15.
23. Catalani A, Bonicelli MG. Kinetics of the curing reaction of a diglycidyl ether of bisphenol A with a modified polyamine. Thermochim Acta. 2005;438:126–9.
24. Vyazoykin S, Mititelu A, Sbirrazzuoli N. Kinetics of epoxy-amine curing accompanied by the formation of liquid crystalline structure. Macromol Rapid Commun. 2003;24:1060–5.
25. Rosu D, Cascaval CN, Mustata F, Ciobanu C. Cure kinetics of epoxy resins studied by non-isothermal DSC data. Thermochim Acta. 2002;383:119–27.
26. Xu G, Shi WF, Shen SJ. Curing kinetics of epoxy resins with hyperbranched polyesters as toughening agents. J Polym Sci Part B Polym Phys. 2004;42:2649–56.
27. Cole KC, Hechler JJ, Noel D. A new approach to modeling the cure kinetics of epoxy/amine thermosetting resins. 2. Application to a typical system based on bis[4-(diglycidylamino)phenyl]methane and bis(4-aminophenyl) sulfone. Macromolecules. 1991;24:3098–4010.
28. Ma ZG, Gao J. Curing kinetics of o-cresol formaldehyde epoxy resin and succinic anhydride system catalyzed by tertiary amine. J Phys Chem B. 2006;110:12380–3.